ChemPlusChem

Research Article
doi.org/10.1002/cplu.202300474

Chemistry Europe
European Chemical Societies Publishing

www.chempluschem.org

Deoxygenation of Oxiranes by $\lambda^3\sigma^3$-Phosphorus Reagents: A Computational, Mechanistic, and Stereochemical Study

Arturo Espinosa Ferao*[a]

Dedicated to Professors Alberto Tárraga and Rainer Streubel on their 70th and 65th birthday, respectively.

The deoxygenation of parent and substituted oxiranes by $\lambda^3\sigma^3$-phosphorus reagents has been explored in detail, therefore unveiling mechanistic aspects as well as regio- and stereochemical consequences. Attack to a ring C atom is almost always preferred over one-step deoxygenation by direct P-to-O attack. In most cases a carbene transfer occurs as first step, leading to a phosphorane and a carbonyl unit that thereafter react in the usual Wittig fashion via the corresponding $\lambda^5\sigma^5$-1,2-oxaphosphetane intermediate. Betaines rarely constitute true minima after the first C-attack to oxiranes, at least in the gas-phase. Use of the heavier derivatives $AsMe_3$ and $SbMe_3$ as oxirane deoxygenating reagents was also mechanistically studied. The thermodynamic tendency of $\lambda^3\sigma^3$-phosphorus reagents to act as oxygen (O-attack) or carbene acceptors (C-attack) was theoretically studied by means of the *thermodynamic oxygen-transfer potential* (TOP) and the newly defined *thermodynamic carbene-transfer potential* (TCP) parameters, that were explored in a wider context together with many other acceptor centres.

Introduction

The highly strained three-membered ring of oxirane (ring strain energy, RSE = 26.55 kcal/mol)[1] and strong polarization of the C–O bonds determine that epoxides **I** (Figure 1) are a class of active chemicals. Methods for deoxygenation of epoxides (oxiranes) to alkenes are of paramount importance both in synthesis[2] and structural determination.[3] Stemming from the seminal report of Sharpless in 1972 using a stoichiometric amount of ^{n}BuLi and WCl_6,[4] a variety of promoters have been developed for the effecttive deoxygenation of epoxides,[5] including phosphanes, silanes, iodides, and heavy metals. The wide-spread use in several deoxygenation and dehydration reactions of $\lambda^3\sigma^3$-phosphorus reagents,[6] namely phosphanes and phosphites, rely on the formation of the P=O bond as the driving force. This includes reduction of nitroso and nitro compounds,[6a,7] as well as the related desulfurization of sulfur-containing compounds such as disulfides.[8] In 1963 Speziale et al.[9] proposed the intermediacy of betaines in the reaction of tertiary phosphanes with epoxides substituted with electron withdrawing groups, due to their equilibrium with phosphoranes and their trapping with external aldehydes. A more detailed study[10] revealed the formation of *cis*- and *trans*-4-octene from the corresponding *cis*- and *trans* oxides, respectively, which could not be explained exclusively by S_N2-type attack of the tertiary phosphane (^{n}Bu$_3$P or Ph$_3$P) to the epoxide C atom. Attack of phosphorus to oxygen was suggested, leading to an intermediate **II** (Figure 1), like that proposed by Denny for episulfides.[11] In 1987 Wong and co-workers stated[12] that the reported deoxygenation of epoxides to olefins[13] might go through the betaine intermediate so that a stereochemical inversion occurs, but without any further evidence. Indeed such a proposal was refuted by theoretical studies showing that at least alkyl-substituted oxiranes eliminate a carbonyl unit, thus behaving as carbene-transfer reagents towards phosphanes, due to the instability of the C–C bond in betaines.[14] Some other P(III) reagents lead to different products, such as chlorohydrin phosphites when using diethylchlorophosphite.[15] FLP (frustrated Lewis pair) combinations of phosphanes with boranes induce ring opening of epoxides affording zwitterionic products **III** (Figure 1), as recently shown by Slootweg.[16] This study reveals the high barrier ($\Delta G^{\ddagger}$ = 44.4 kcal/mol) computed (ωB97X-D/6-31G**) for ring opening by direct P-attack of ^{t}Bu$_2$P-CH$_2$-BPh$_2$ to the less substituted ring C atom of methyl oxirane. Instead, epoxide ring activation by the acidic boron centre

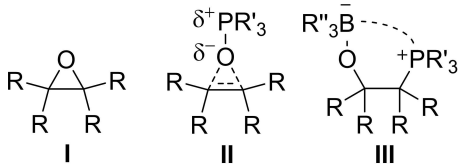

Figure 1. Proposed structures.

[a] *Prof. Dr. A. Espinosa Ferao*
Departamento de Química Orgánica
Universidad de Murcia
Campus de Espinardo
30071 Murcia (Spain)
E-mail: artuesp@um.es

Supporting information for this article is available on the WWW under https://doi.org/10.1002/cplu.202300474

Part of a Special Collection: "From Light to Heavy: Advancing the Chemistry of Pnictogen Compounds"

($\Delta G^{\neq} = +4.3$ kcal/mol) facilitates ring opening by nucleophilic C-attack from a second molecule of the FLP species ($\Delta\Delta G^{\neq} =$ 11.8 kcal/mol; $\Delta\Delta G = -23.5$ kcal/mol), which thereafter intramolecularly replaces the initial activating molecule ($\Delta\Delta G^{\neq} =$ 16.3 kcal/mol; $\Delta\Delta G = -16.4$ kcal/mol).

The analogous desulfurization reaction of thiiranes[11] by tervalent phosphorus reagents was recently studied computationally[17] and the existence of two different transition states (TSs) from the direct P···S interaction was demonstrated. For twelve PZ_3 reagents analyzed in the desulfurization of parent thiirane, a lowest barrier TS ($\Delta G^{\neq} = 19.9$ to 30.3 kcal/mol) was found for the nucleophilic P-to-S attack, whereas in some cases a second higher-energy TS ($\Delta G^{\neq} = 61.9$ to 68.9 kcal/mol) corresponding to the inverse S-to-P attack could be located. The alternative three-step desulfurization, initiated by nucleophilic attack to the ring C atom followed by cyclization of the thiobetaine and [2+2]-cycloreversion of the 1,2-thiaphosphetane exhibited higher barrier for the first rate-determining step than the direct P-to-S attack.

As briefly mentioned above, the driving force for the oxirane deoxygenation reaction is a consequence of both the relief of oxirane RSE and the exothermicity of the P(III)→P(V) oxidation process, which was defined against the H_2O_2/H_2O redox couple via the thermodynamic oxygen transfer potential (TOP) parameter and computed for a small set of oxophilic reagents.[18] The analogous thermodynamic sulphur transfer potential (TSP) parameter[17] was studied for a wider set of reducing (thiophilic) reagents and defined relative to the S_8/S_7 redox couple instead of using gaseous (or solvated) S atoms arising from the solid element.[19] Recently, Kepp reported a quantitative scale for atomic oxo- and thiophilicity and showed that oxophilicity inversely correlates with electronegativity and also with the effective nuclear charge.[20]

Herein a comprehensive high-level computational mechanistic study of the deoxygenation reaction of oxirane with $\lambda^3\sigma^3$-phosphorus reagents is presented, together with studies in representative substituted oxiranes with alkyl or electron withdrawing groups. A comparison with heavier $\lambda^3\sigma^3$-pnictogen derivatives R_3Pn (Pn = As, Sb) is included. A ranking of oxophilicity for a wide set of reducing agents by means of their computed TOP is presented and compared to a newly defined *thermodynamic carbene-transfer potential* (TCP) parameter.

Results and Discussion

Deoxygenation of parent oxirane

The reaction of parent oxirane (**1 a**) with three different PZ_3 reagents (**2**), for Z = Me (**a**), OMe (**b**) and Cl (**c**), were studied as representative cases of $\lambda^3\sigma^3$-phosphorus compounds, at the DLPNO-CCSD(T)/def2-QZVPP//B3LYP-D4/def2-TZVP level of theory (see Computational Details). Two different mechanistic pathways were found in all three cases. The direct P-to-O attack affords ethylene (**3 a**) and the P-oxide derivative (**4**). On the other hand, the good leaving group ability of the carbonyl subunit (**7 a**) favours P-to-C attack that results in carbene transfer leading to the corresponding phosphorane (**6**) (Scheme 1). As previously reported,[14] the betaine (**5**) intermediate rarely constitutes a local minimum and readily decomposes into **6** and **7**, over a very low barrier (often not located) transition state (TS). Thereafter, a normal Wittig reaction occurs via the usual 1,2-oxaphosphetane (OP) intermediates (**8**)[14] with the O atom sequentially in axial ($\mathbf{8^{ax}}$) and equatorial ($\mathbf{8^{eq}}$) positions around P and finally decomposing into ethylene (**3 a**) and the P-oxide (**4**) (Scheme 1).

In case of trimethyl phosphane (**2 a**), the located "betaine" in the gas phase has rather a **6 a·7 a** van der Waals complex structure ($d_{C\cdots C} = 2.592$ Å; $d_{P\cdots O} = 3.382$ Å). Only when including solvent effects, such as THF or acetonitrile, a proper betaine **5 a**, with rather elongated (weak) covalent C–C bonds (1.794 and 1.798 Å, respectively), was located in the potential energy surface (PES). According to the positive electric charge at the PMe_3 fragment (q = 0.268 e, either Mulliken or Löwdin) and the increase in positive charge at the P atom ($\Delta q^{Mull} = 0.178$ e) compared to O ($\Delta q^{Mull} = 0.047$ e) in the TS for the direct **1 a** + **2 a** → **3 a** + **4 a** process, this must result from P-to-O nucleophilic attack (*O*-attack pathway in Scheme 1). The latter is much higher in energy than the TS for the first (rate-determining) step of the preferred *C*-attack pathway ($\Delta\Delta G^{\neq}_{O/C} = 9.33$ kcal/mol) (Figure 2).

The latter furnishes trimethyl methylene phosphorane (**6 a**) and formaldehyde (**7 a**) which then undergo Wittig olefination through consecutive axial (O position around P) and equatorial

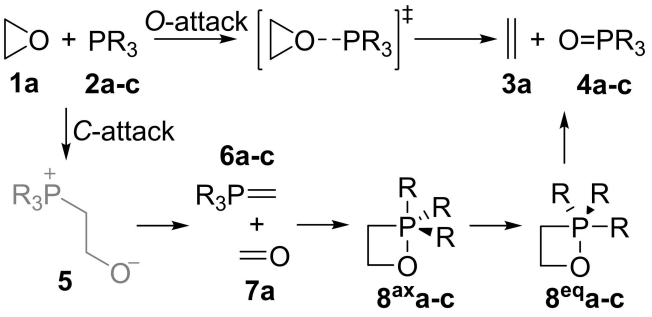

Scheme 1. Mechanistic pathways for the deoxygenation of parent oxirane **1 a** with P(III) reagents **2** (**a**, R = Me, **b**, R = OMe; **c**, R = Cl).

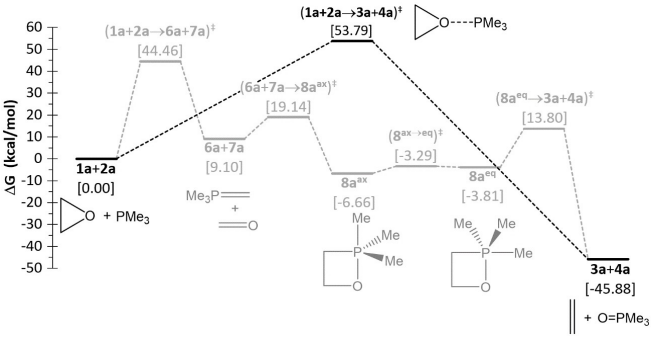

Figure 2. Computed (DLPNO-CCSD(T)/def2-QZVPP//B3LYP-D4/def2-TZVP) relative Gibbs energy profile for the deoxygenation of oxirane (**1 a**) with trimethyl phosphane (**2 a**).

OPs, in good agreement with previous theoretical studies at lower[21] or similar[22] computational levels.

Similar results were obtained for the oxirane deoxygenation using methyl phosphite (**2b**) (Figure S1) or phosphorus trichloride (**2c**), although the energy difference for the rate determining steps for the *O* vs *C*-attack decreases ($\Delta\Delta G^{\ddagger}_{O/C}$ = 2.91 and −0.07 kcal/mol, respectively), so that the direct *O*-attack turns out to be slightly preferred in case of PCl_3 (Figure 3). In case of PF_3 (**2d**, not shown), the O-attack ($\Delta G^{\ddagger}_{O}$ = 53.02 kcal/mol) and carbene transfer pathways ($\Delta G^{\ddagger}_{C}$ = 53.01 kcal/mol) are equally kinetically unfavoured although the overall deoxygenation process is highly exergonic.

The TSs for the C- and O-attack with PCl_3 and PF_3 exhibits some multireference character and were therefore evaluated at the CASSCF-MRACPF/def2-SVPD level (see the Computational Details), showing essentially an increased preference for the O-attack, compared to the single-reference method: $\Delta G^{\ddagger}_{O/C}$ = 50.16/54.11 and 47.75/53.01 kcal/mol for PCl_3 and PF_3, respectively. It should also be noted the decreasing overall exothermicity for the deoxygenation of the same oxirane (**1a**) substrate on moving from trimethyl phosphite **2b** ($\Delta G^{\ddagger}$ = −62.26 kcal/mol, Figure S1) to phosphorus trifluoride **2d** (ΔG = −47.83 kcal/mol), to trimethyl phosphane **2a** ($\Delta G^{\ddagger}$ = −45.88 kcal/mol, Figure 2) and to phosphorus trichloride **2c** ($\Delta G^{\ddagger}$ = −39.11 kcal/mol, Figure 3), which should be related to some decreasing oxophilicity in the series $P(OMe)_3 > PF_3 > PMe_3 > PCl_3$ (*vide infra*).

Deoxygenation of substituted oxiranes

Next, the reaction of two 2,3-disubstituted symmetrical and non-symmetrical oxiranes with PMe_3 (**2a**), as prototypical P(III) deoxygenation reagent, were studied with emphasis in the stereochemical outcome and regioselectivity. Both 2,3-disubstituted oxiranes were chosen with *trans* configuration, although the conclusion could be easily extrapolated to the *cis* configured counterparts.

First, deoxygenation of *trans*-2,3-dimethyl-oxirane (**1b**) was explored. As expected, direct *O*-attack led to the most stable *E*-configured 2-butene (**3b^{E}**) over the highest TS. Carbene transfer via *C*-attack has lower energy barrier and furnishes the methyl-substituted trimethyl ethylenphosphorane (**6d**) and acetaldehyde (**7b**), that subsequently undergo normal (lithium-free) Wittig olefination reaction (Figure 4). The *threo*-OP (only axial O pseudorotamers were found) is the most stable one and its TS for formation and decomposition are lower in energy than those corresponding to the *erythro* isomer, thus explaining the experimentally observed preferential formation of the *E*-olefin in case of trimethyl phosphoranes.[21] However, it is worth noting that decomposition of the less stable (less abundant) *erythro*-OP (**8d^{eryt}**) is somewhat faster ($\Delta\Delta G^{\ddagger}$ = 23.08 kcal/mol) than the *threo* (**8d^{thre}**) isomer ($\Delta\Delta G^{\ddagger}$ = 23.83 kcal/mol).

When the oxirane is not equally substituted at both ring C atoms, the potential energy surface is far more complicated due to possible attack of the P(III) reagent not only at O but also at both (different) C centres, and this is the case for *trans*-2-cyano-3-methyl-oxirane (**1c**) (Figure 5).

Direct attack of PMe_3 (**2a**) to the O atom has two possible orientations, the one with the P centre aligned with the O–C2 endocyclic bond (C2 stands for the ring C atom bearing the CN substituent) being favoured by 8.44 kcal/mol.

The preferred (lowest energy) pathway starts by P-attack to C3 promoting ring opening to give a betaine (**5b^{eryt}**) that furnishes the *erythro*-OP (**8f^{eryt}**) and finally decomposes to *trans*-2-butenenitrile (**3c^{E}**) (Figure 5). Betaine **5b^{eryt}** can also undergo C–C bond cleavage affording the methyl-substituted phosphorane (**6d**) and formyl cyanide (**7c**) that, subsequently can undergo Wittig reaction following the two possible topological (*ul* or *lk*) approaches leading, to the above mentioned *erythro*-OP (**8f^{eryt}**) (path not shown) or to the *threo* diastereomer (**8f^{thre}**), respectively, the latter furnishing the slightly most stable *cis*-2-butenenitrile (**3c^{Z}**). The other possible attack of PMe_3 (**2a**) to the ring C2 position of **1c** is slightly unfavoured compared to C3-attack and results in carbene transfer affording cyano-methyl-enphosphorane (**6e**) and acetaldehyde (**7b**) as starting point for a new Wittig reaction pathway via regioisomeric less stable OPs (**8e**) (Figure 5). It should be noted that decomposition (retro-cycloaddition) of the latter is (again) faster for the less stable *erythro* ($\Delta\Delta G^{\ddagger}$ = 7.46 kcal/mol) than for the *threo* ($\Delta\Delta G^{\ddagger}$ = 7.90 kcal/mol) diastereomer.

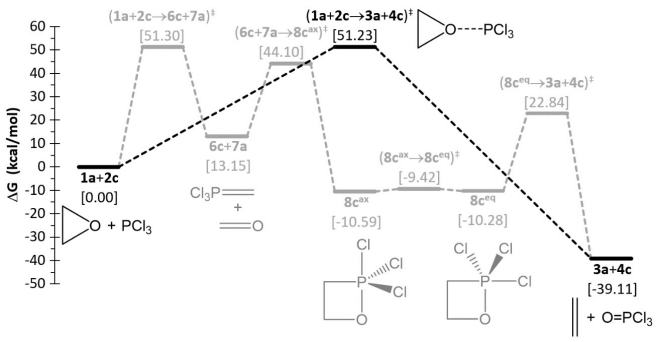

Figure 3. Computed (DLPNO-CCSD(T)/def2-QZVPP//B3LYP-D4/def2-TZVP) relative Gibbs energy profile for the deoxygenation of oxirane (**1a**) with phosphorus trichloride (**2c**).

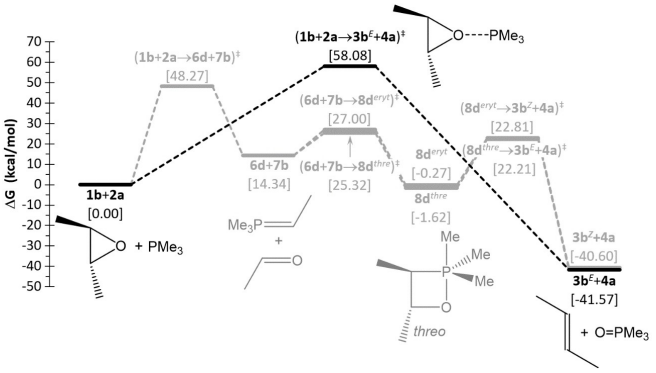

Figure 4. Computed (DLPNO-CCSD(T)/def2-QZVPP//B3LYP-D4/def2-TZVP) relative Gibbs energy profile for the deoxygenation of *trans*-2,3-dimethyl-oxirane (**1b**) with trimethyl phosphane (**2a**).

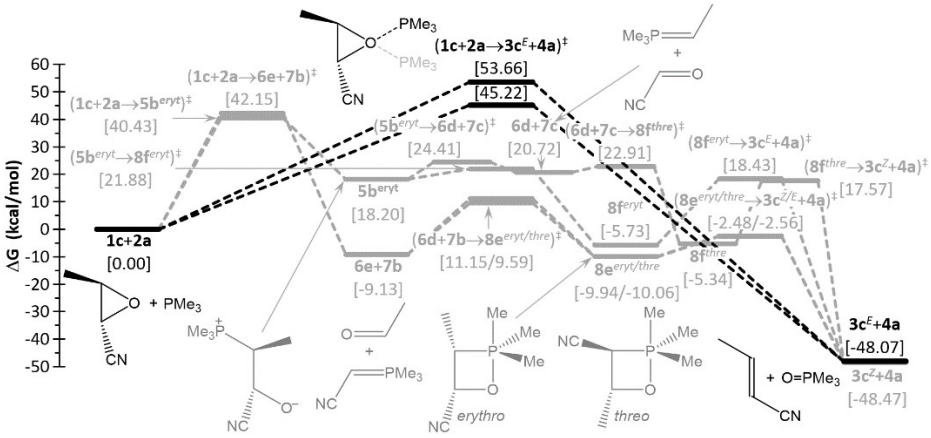

Figure 5. Computed (DLPNO-CCSD(T)/def2-QZVPP//B3LYP-D4/def2-TZVP) relative Gibbs energy profile for the deoxygenation of *trans*-2-cyano-3-methyl-oxirane (**1c**) with trimethyl phosphane (**2a**).

Deoxygenation with heavier $\lambda^3\sigma^3$-pnictogen reagents

The above shown deoxygenation of oxiranes with $\lambda^3\sigma^3$-phosphorus reagents was finally compared to heavier pnictogen analogues $AsMe_3$ (**9a**) and $SbMe_3$ (**9b**), using parent oxirane (**1a**) for the sake of simplicity. With both reagents the direct *O*-attack is higher in energy than the corresponding *C*-attack pathways (Figures 6 and 7) and higher than in case of the lighter analogue PMe_3 (**2a**) (Figure 2). The overall thermochemistry of the deoxygenation process with $PnMe_3$ reagents changes from very exergonic for P (Figure 3) to moderately exergonic for As (Figure 6) and slightly endergonic for Sb (Figure 7), which speaks for a decreasing oxophilicity for $\lambda^3\sigma^3$-pnictogen reagents in the order P > As > Sb (*vide infra*).

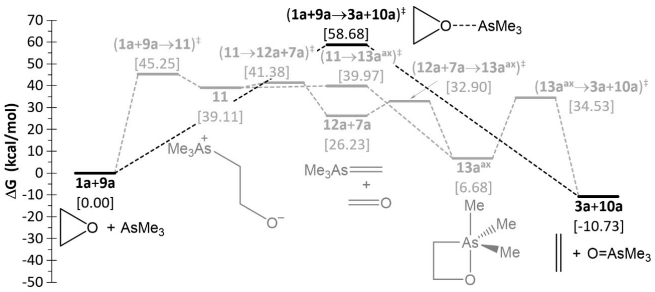

Figure 6. Computed (DLPNO-CCSD(T)/def2-QZVPP(ecp)//B3LYP-D4/def2-TZVP(ecp)) relative Gibbs energy profile for the deoxygenation of oxirane (**1a**) with $AsMe_3$ (**9a**).

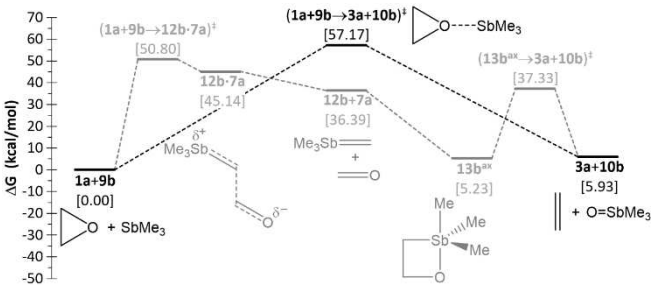

Figure 7. Computed (DLPNO-CCSD(T)/def2-QZVPP(ecp)//B3LYP-D4/def2-TZVP(ecp)) relative Gibbs energy profile for the deoxygenation of oxirane (**1a**) with $SbMe_3$ (**9b**).

The alternative C-attack of $AsMe_3$ (**9a**) constitutes the minimum energy pathway and initially provides, even in the gas-phase, a true betaine minimum (**11**) with an elongated yet covalent C–C bond (1.611 Å). The almost barrierless C–C bond rotation provides the four membered λ^5-1,2-oxaarsetane ring (**13a^{ax}**, Figure 6), analogous to the genuine Wittig reaction intermediate (**8a**, Figure 2). The weakness of the C–C bond in **11** (Mayer bond order,[23] MBO = 0.750) determines the very easy low barrier ($\Delta\Delta G^{\neq}$ = 2.27 kcal/mol) dissociation into the carbonyl unit **7a** and methylene-$\lambda^5\sigma^5$-arsane **12a**, which are the required components for an arsa-Wittig[24] reaction via the same intermediate **13a^{ax}** (Figure 6). No equatorial pseudorotamer **13a^{eq}** was located in the PES.

In case of $SbMe_3$ (**9b**) the C-attack is qualitatively similar although furnishes the carbene transfer methylene-$\lambda^5\sigma^5$-stibane **12b** intermediate via a van de Waals complex intermediate **12b·7a** ($d_{C\cdots C}$ = 2.681 Å; MBO < 0.1). The stiba-Wittig reaction of **12b** and aldehyde **7a** is globally exergonic although [2 + 2] cycloreversion of the $\lambda^5\sigma^5$-1,2-oxastibetane[25] intermediate (**13b^{ax}**) turns out to be endergonic, most likely due a decreased stability of the Pn=O bond in case of As (*vide infra*). Therefore, **13b^{ax}** is expected to be final (most stable) product (Figure 7).

The relative easiness for the [2 + 2] cycloreversion seems not to be connected to instability of the corresponding $\lambda^5\sigma^5$-1,2-oxapnictogenetane in terms of their ring strain energy (RSE), that were computed to be very similar for all three different pnictogens: 9.37 kcal/mol for **8a^{ax}** (P) (reported value 9.08 kcal/mol),[22] 8.81 kcal/mol for **13a^{ax}** (As) and 9.02 kcal/mol for **13b^{ax}** (Sb).

Oxygen atom and carbene group transfer ability

The above-mentioned decreasing deoxygenation ability for $PnMe_3$ reagents on descending group 15 (P > As > Sb), as well as within $\lambda^3\sigma^3$-phosphorus reagents in the order $P(OMe)_3$ > PF_3 > PMe_3 > PCl_3, is related to some oxophilic property of the

reducing PnR_3 species and their thermodynamic tendency to form the corresponding oxidized $O{=}PnR_3$ products. This relative trend to uptake an O atom from oxirane or any other *O*-atom donor was reported for a small set of compounds, by means of the *Thermodynamic Oxygen (atom transfer) Potential* (TOP)[18] and referred towards the H_2O_2/H_2O redox (*O*-donor/acceptor) couple. A similar scale for the sulphur atom transfer ability (TSP) was later reported using the S_8/S_7 couple as reference.[17]

Herein a wide set of acceptor compounds "B:" bearing either an atomic lone pair (LP) or an unsaturation that is prone to oxidation by oxygen atom transfer are studied using state-of-the-art single-reference computational methods, by evaluation of the enthalpy change corresponding to the reaction $B{:}+H_2O_2 \rightarrow B{=}O + H_2O$ (Figure 8). Obviously, according to this definition, the couple H_2O_2/H_2O used as reference has $TOP^H = 0.0$ kcal/mol. The "H" superscript refers to the fact that enthalpy changes are used instead of zero-point corrected energies as employed in some preliminary reports (although differences are rather small). The most negative the TOP is, the higher the *O*-acceptor character of the left side compound (*O*-acceptor) of any given couple. Hence, the *O*-acceptor of any couple is thermodynamically able to uptake the O atom from any oxidized form (right side, *O*-donor) of any other couple placed below (less negative TOP) in the scale. Therefore, oxirane can be reduced to ethylene (highlighted in blue in Figure 8) by almost any PR_3 reagent (including cyclic derivatives), several model free and complexed phosphinidenes, carbon monoxide,[26] isocyanides and NHCs (exemplified by 1,3-dimethyl-2-imidazolydene, I^{Me2}). Also, methylene-λ^5-phosphane and $AsMe_3$ could do the job, although with low exothermicity.

One of the most striking results is the one obtained for the unstable molecule of carbon monosulphide,[27] which turns out to be an exceptionally powerful *O*-acceptor (Figure 8), in line with its reported very high *S*-acceptor character.[17] Trimethyl phosphite is also very powerful *O*-acceptor immediately followed by phosphinidenes and NHCs. In general, the other

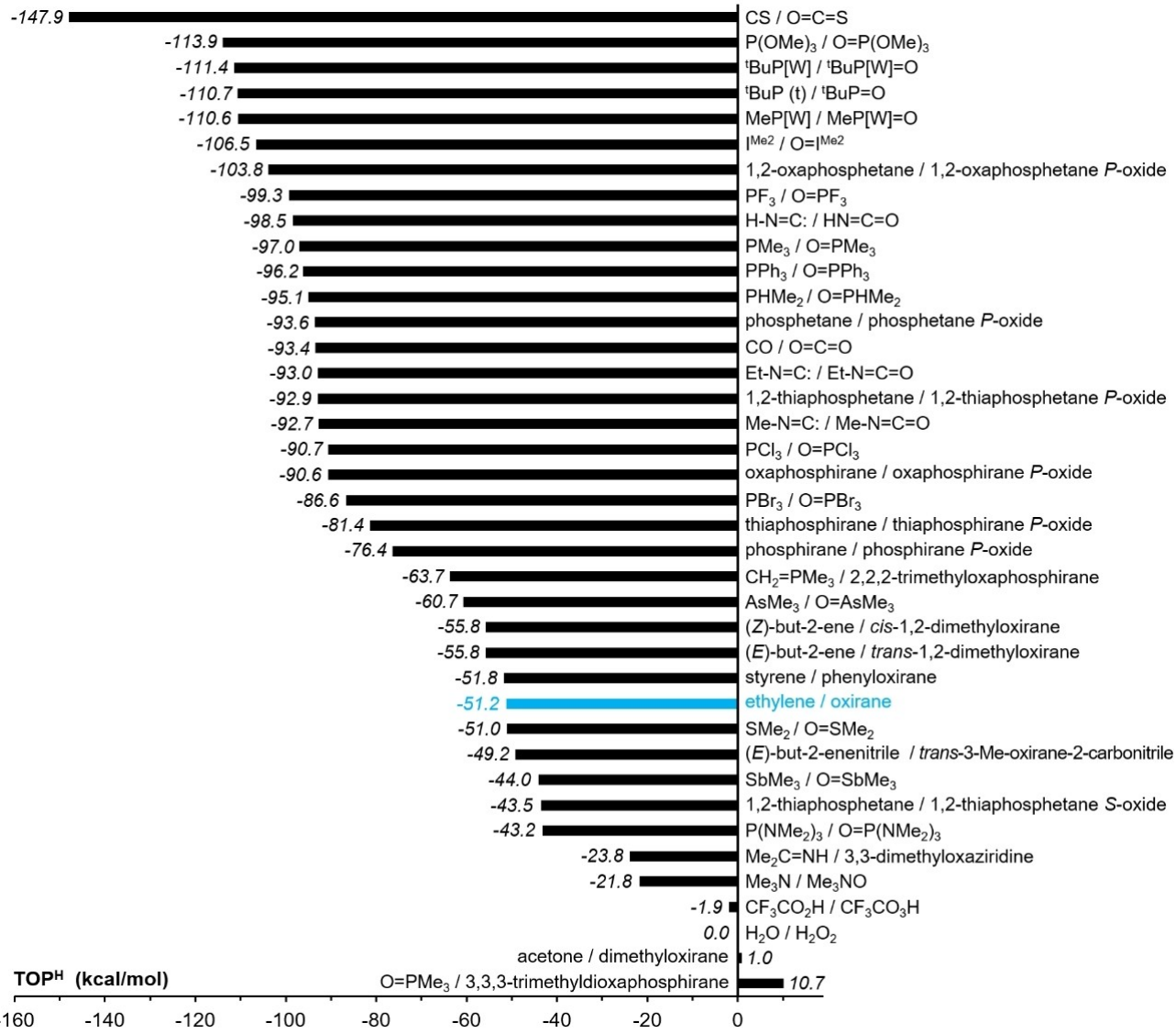

Figure 8. Computed (DLPNO-CCSD(T)/def2-QZVPP(ecp)//B3LYP-D4/def2-TZVP(ecp)) thermodynamic *O*-transfer potentials.

typical symmetric P(III) reagents are next placed, in the order $PF_3 > PMe_3 > PPh_3 > PCl_3 > PBr_3 \gg P(NMe_2)_3$, the latter (hexamethyl phosphorous triamide, HMPT) being, an exceptional case with very reduced *O*-acceptor ability. The significantly lower (absolute) TOC value in phosphirane compared to the analogous acyclic phosphanes is likely due to the mechanism used by phosphirane to relieve ring strain by increasing the s character of the LP at the P atom,[1] thus becoming more difficult to oxidise, and has also been reported to influence its higher pyramidal inversion barrier.[28] However, *N*- and *S*-electron donor centres, $SbMe_3$ (*vide supra*, Figure 7) and the π-bonds of the C=N and C=O groups are very poor *O*-acceptors and indeed, oxidized forms of the latter, oxaziridines[29] and dioxiranes,[30] respectively, are employed as useful oxidants.

On the other hand, the different behaviour shown by $\lambda^3\sigma^3$-phosphorus reagents towards oxirane show that they can not only act as deoxygenation reagents but can also promote *C*-attack, thus behaving as carbene acceptor centres. Therefore, like TOP, it is interesting to define a *thermodynamic carbene (group) transfer potential* (TCP) to measure this ability.

A molecular species displaying carbene group transfer ability is 2,2,2-trimethyloxaphosphirane (TMOP), that was reported as intermediate in the PMe_3-mediated reductive dimerization of carbonyl compounds to olefins.[14] Its high performance as carbene group (H_2C:) donor is due to the good leaving group ability of the $O{=}PMe_3$ fragment and the moderately high RSE computed for TMOP (16.93 kcal/mol), using the same type of appropriate homodesmotic reactions employed for other three-membered rings,[1,31] somewhat lower to that reported for the parent $\lambda^5\sigma^5$-oxaphosphirane (24.08 kcal/mol).[32] The TCP for any potential carbene acceptor species "B:" is obtained upon enthalpy change evaluation for the reaction depicted in Scheme 2.

The resulting TCP values (Figure 9) measure the relative tendency of accepting a carbene unit from TMOP.

Again, carbon monosulphide, the different model phosphinidenes and NHCs display the highest (most negative) TCP values. The next group in decreasing carbene-acceptor ability contains isocyanides and olefin π-bonds, followed by P(III) reagents which display a wide range of TCP values, with the best carbene acceptors being $P(OMe)_3$ and $P(NMe_2)_3$. Imine and carbonyl π-bonds display moderate TCP values, whereas the lowest values correspond to As:, S:, Sb: and N: centres (Figure 9). The minimum value TCP = 0.00 kcal/mol corresponds to the $O{=}PMe_3$/TMOP couple, thus $O{=}PMe_3$ being the weakest carbene acceptor and 2,2,2-trimetil-oxaphosphirane (TMOP) the strongest carbene donor. A slightly lower carbene donor character was found for 2,2,2-tris(methoxy)oxaphosphirane (TCP = −0.6 kcal/mol, not included in Figure 9), with $O{=}P(OMe)_3$ being the carbene-acceptor partner.

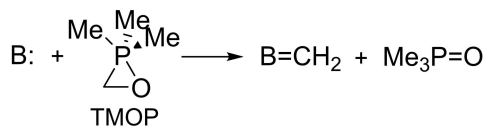

Scheme 2. Reference reaction for evaluating TCP.

As pointed out in the mechanistic studies of oxirane deoxygenation, the preferred pathway is the result of the kinetic preference for the O- *versus* C-attack for any given pnictogen(III) reagent. Assuming that there might be some relationship between the kinetic and thermodynamic preferences, it is worth comparing thermodynamic oxygen-transfer (TOP) with carbene-transfer (TCP) potentials. From the TOP vs TCP plot it becomes obvious some roughly linear (or, most properly, second-order polynomial) correlation showing an increase in "transfer" ability according to the central acceptor atom bearing an atomic LP, following the order: N: < Sb: < S: < As: < P: < C: (Figure 10). Phosphinidenes lie well apart from the other phosphorus centred acceptors with a remarkably enhanced carbene-acceptor ability compared to the best oxygen-acceptor. Also, hexamethyl phosphorous triamide (HMPT), $P(NMe_2)_3$, falls well outside the typical region for phosphorus centred acceptors, owing to its highly decreased *O*-acceptor ability compared to its rather high carbene-acceptor features (in line with other highly basic phosphane derivatives).

The family of π-bond acceptors (C=X) falls in a well-separated region with moderate carbene-acceptor but very low O-acceptor properties and displaying a roughly linear correlation following the order C=O < C=N < C=C (Figure 10). Triads H_2O_2/H_2O/MeOH and CF_3CO_3H/CF_3CO_2H/CF_3COOMe fall in the very low TOC part of the plot.

Conclusions

Oxiranes can undergo deoxygenation to olefins using typical $\lambda^3\sigma^3$-phosphorus reagents such as trymethyl phosphite and alkyl- or aryl-phosphanes. Most often (excluding HMPT) there exists a one-step pathway proceeding by direct P-to-O attack. However, the lowest energy pathway (except for PCl_3) is the one involving C-attack and promoting, in the most general case, carbene transfer leading to a methylene phosphorane and a carbonyl unit. These two molecular fragments then react in the normal Wittig fashion leading to an olefin and phosphane oxide via the corresponding 1,2-oxaphosphetane intermediate. A betaine resulting from the direct C-attack of the phosphane to oxirane can only exceptionally be located as a minimum in the gas-phase but its existence is favoured in polar solvents. In the reaction of substituted phosphoranes with aldehydes, formation of the most stable *threo*-1,2-oxaphosphetane is favoured, thus preferentially leading to the most stable *E*-alkene. However, the experimental observed preference for the *Z*-alkene in some cases could be explained by the faster decomposition of the *erythro*- compared to the *threo*-1,2-oxaphosphetane, which seems to be a general behaviour. In 2,3-disubstituted oxiranes with one electron withdrawing substituent (at C2), the preferred pathway starts by C3-attack leading to a betaine that furnishes the corresponding 1,2-oxaphosphetane by low-barrier C–C bond rotation. The use of heavier analogues $AsMe_3$ and $SbMe_3$ produce qualitatively similar results, although the deoxygenation is less favoured both kinetically and thermodynamically, being an endergonic process in case of $SbMe_3$.

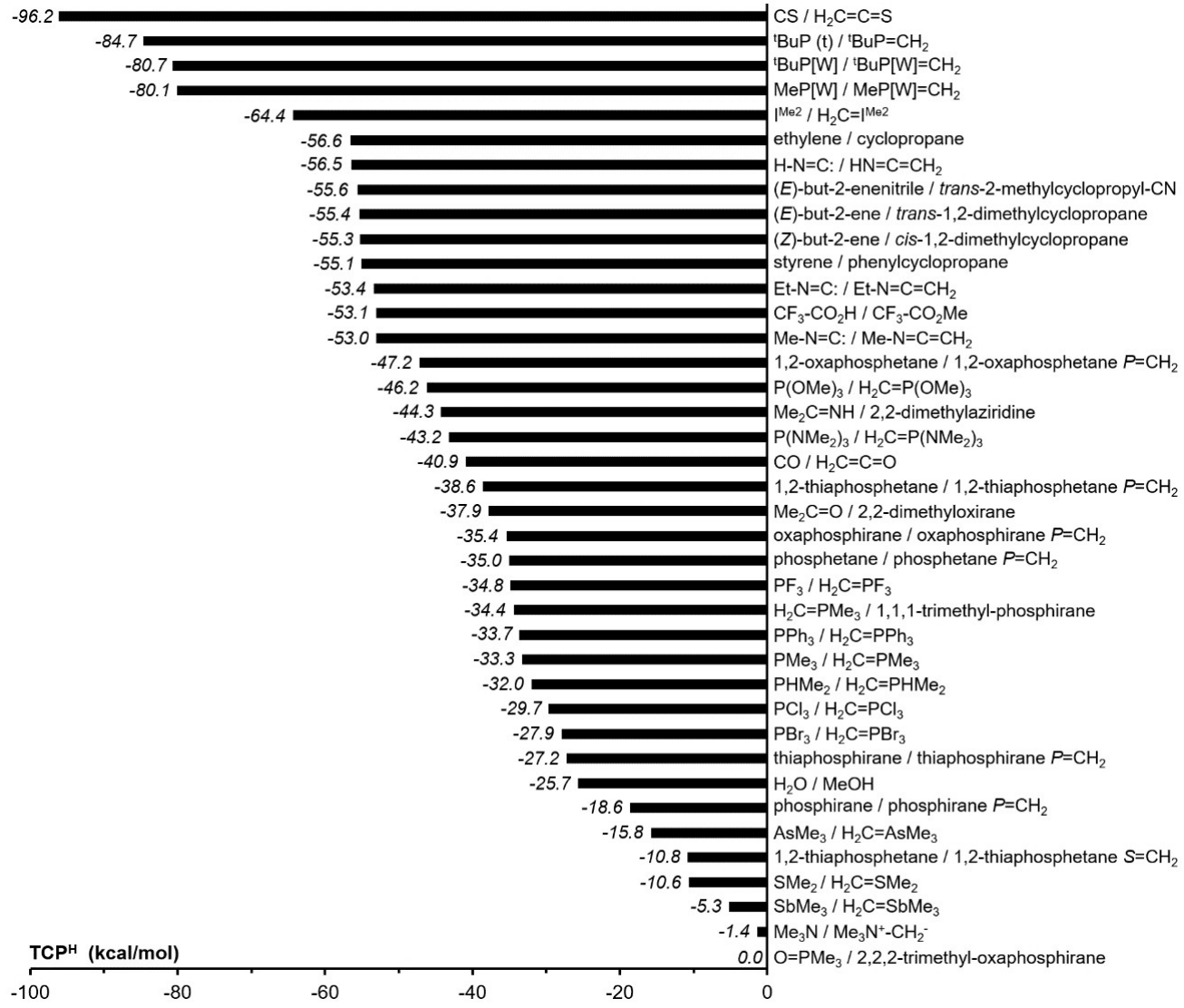

Figure 9. Computed (DLPNO-CCSD(T)/def2-QZVPP(ecp)//B3LYP-D4/def2-TZVP(ecp)) thermodynamic carbene-transfer potentials.

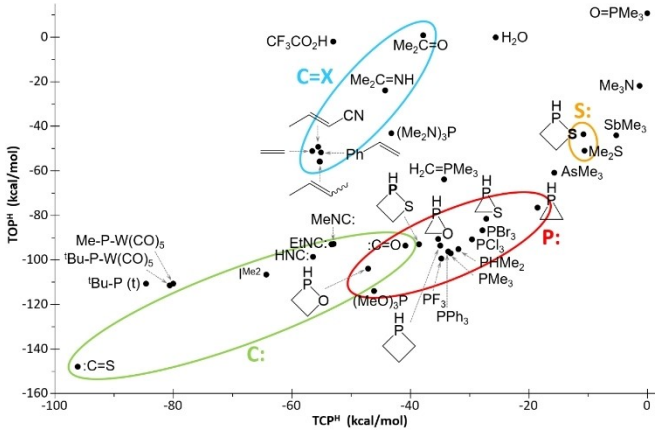

Figure 10. Computed (DLPNO-CCSD(T)/def2-QZVPP(ecp)//B3LYP-D4/def2-TZVP(ecp)) plot of thermodynamic oxygen versus carbene-transfer potentials.

The ability to uptake an oxygen atom has been studied for a variety of O-acceptors by means of the *thermodynamic oxygen-transfer potential* (TOP) and compared with the tendency displayed by the same centres to uptake a carbene unit. The latter is quantified by the newly defined *thermodynamic carbene-transfer potential* (TCP). For typical $\lambda^3\sigma^3$-phosphorus reagents, the *O*-acceptor ability varies in the order $P(OMe)_3 > PF_3 > PMe_3 > PPh_3 > PCl_3 > PBr_3 \gg P(NMe_2)_3$, the latter featuring lower -TOP than olefins and thus resulting thermodynamically unable to promote deoxygenation of oxiranes. The TOP scale also reveals phosphinidenes and carbenes (typically NHCs, isocyanides and carbon monoxide) as powerful *O*-acceptors. In general, the O-acceptor ability (TOC) correlates with the carbene-acceptor properties (TCP), a remarkable exception being $P(NMe_2)_3$ that keeps some moderate carbene-acceptor ability despite its low -TOC. The same holds for π-bonds in C=X species (X: C, N, O) that display reduced O-acceptor but moderately high carbene-acceptor properties.

Experimental Section

Computational details: DFT calculations were performed with the ORCA electronic structure program package.[33] All geometry optimizations were run in redundant internal coordinates, with tight convergence criteria using the B3LYP functional[34] together with the def2-TZVP basis set[35] and speeded up by means of the fast and accurate "chain of spheres" RIJCOSX algorithm.[36] The latest Grimme's semiempirical atom-pairwise dispersion correction based on tight binding partial charges (DFT-D4) was included in all calculations.[37] Harmonic frequency calculations verified the nature of the computed species featuring none or only one negative eigenvalues for minima or transition states (TSs), respectively. The later were checked by performing intrinsic reaction coordinate calculations.[38] Only when explicitly indicated, solvent effects were included by means of the conductor-like polarizable continuum model (CPCM).[39] Energy values were corrected for the Gibbs free energy correction term at the optimization level and obtained by the DLPNO method[40] for the "coupled cluster" level with single, double as well as triple perturbatively introduced excitations (CCSD(T))[41] and the def2-QZVPP basis set.[35] In almost all CCSD(T) calculations, the T1 diagnostic was below 0.018 (normally below 0.013) hence assuming negligible multireference character. For the only four TS structures displaying T1 diagnostic in the range 0.022–0.024, the energies were recomputed using the CASSCF method[42] with the multireference average coupled-pair functional (MRACPF) approach[43] and the def2-SVPD basis set.

Supporting Information

Additional file containing the computed Gibbs energy profile for the deoxygenation of **1a** with **2b**, as well as the Cartesian coordinates and energies for all computed species.

Acknowledgements

The computational resources used at the *Servicio de Cálculo Científico* (SCC – University of Murcia) computation centre are deeply acknowledged.

Conflict of Interests

The author declares no conflict of interest.

Data Availability Statement

The data that support the findings of this study are available in the supplementary material of this article.

Keywords: carbene-transfer · deoxygenation · DFT calculations · oxiranes · pnictogens

[1] A. Rey Planells, A. Espinosa Ferao, *Inorg. Chem.* **2020**, *59*, 11503–11513.
[2] *E.g.* a) J. W. Cornforth, R. H. Cornforth, K. K. Mathew, *J. Chem. Soc.* **1959**, *112*, 2539; b) S. F. Erady, M. A. Ilton, W. S. Johnson, *J. Am. Chem. Soc.* **1968**, *90*, 2882; c) E. J. Corey, W. G. Su, *J. Am. Chem. Soc.* **1987**, *109*, 7534–7536; d) G. A. Kraus, P. J. Thomas, *J. Org. Chem.* **1988**, *53*, 1395–1397; e) W. S. Johnson, M. S. Plummer, S. P. Reddy, W. R. Bartlett, *J. Am. Chem. Soc.* **1993**, *115*, 515–521; f) D. M. Nowak, P. T. Lansbury, *Tetrahedron* **1998**, *54*, 319–336; g) M. J. Krische, B. M. Trost, *Tetrahedron* **1998**, *54*, 7109–7120; h) J. Johnson, S.-H. Kim, M. Bifano, J. DiMarco, C. Fairchild, J. Gougoutas, F. Lee, B. Long, J. Tokarski, G. Vite, *Org. Lett.* **2000**, *2*, 1537–1540; i) H.-J. Pyun, M. Fardis, J. Tario, C. Y. Yang, J. Ruckman, D. Henninger, H. Jin, C. U. Kim, *Bioorg. Med. Chem. Lett.* **2004**, *14*, 91–94; j) G. A. Molander, D. J. St. Jean Jr., J. Haas, *J. Am. Chem. Soc.* **2004**, *126*, 1642–1643; k) M. Inoue, S. Hatano, M. Kodama, T. Sasaki, T. Kikuchi, M. Hirama, *Org. Lett.* **2004**, *6*, 3833–3836; l) A. B. Smith III, E. F. Mesaros, E. A. Meyer, *J. Am. Chem. Soc.* **2005**, *127*, 6948–6949; m) T. Sengoku, S. Xu, K. Ogura, Y. Emori, K. Kitada, D. Uemura, H. Arimoto, *Angew. Chem. Int. Ed.* **2014**, *53*, 4213–4216.
[3] *E.g.* D. B. Borders, P. Shu, J. E. Lancaster, *J. Am. Chem. Soc.* **1972**, *94*, 2540–2541.
[4] K. B. Sharpless, M. A. Umbreit, M. T. Nieh, T. C. Flood, *J. Am. Chem. Soc.* **1972**, *94*, 6538–6540.
[5] R. C. Larock, *Comprehensive Organic Transformations*; Wiley, New York, **1999**, p. 272, and references cited therein.
[6] a) J. I. G. Cadogan, *Q. Rev. Chem. Soc.* **1968**, *22*, 222–251; b) D. J. H. Smith, in *Comprehensive Organic Chemistry* (Eds. D. H. R. Barton, W. D. Ollis), Pergamon Press, Oxford, **1979**, pp. 1127–1188; c) D. E. C. Corbridge, *Phosphorus. An Outline of its Chemistry, Biochemistry and Uses*, Studies in Inorganic Chemistry 20, Elsevier, Amsterdam, **1995**, p. 319–320 and 352–354.
[7] R. J. Sundberg, *J. Org. Chem.* **1965**, *30*, 3604–3610.
[8] a) R. E. Humphrey, J. L. Potter, *Anal. Chem.* **1965**, *37*, 164–165; b) O. Dmitrenko, C. Thorpe, R. D. Bach, *J. Org. Chem.* **2007**, *72*, 8598–8307.
[9] A. J. Speziale, D. E. Bissing, *J. Am. Chem. Soc.* **1963**, *85*, 3878–3884.
[10] D. E. Bissing, A. J. Speziale, *J. Am. Chem. Soc.* **1965**, *87*, 2683–2690.
[11] M. J. Boskin, D. B. Denny, *Chem. Ind. (London)* **1959**, 330–331.
[12] H. N. C. Wong, C. C. M. Fok, T. Wong, *Heterocycles* **1987**, *26*, 1345–1382.
[13] a) G. Wittig, W. Haag, *Chem. Ber.* **1955**, *88*, 1654–1666; b) K. Yamada, S. Goto, H. Nagase, Y. Kyotani, Y. Hirata, *J. Org. Chem.* **1978**, *43*, 2076–2077; c) Z. Paryzek, R. Wydra, *Tetrahedron Lett.* **1984**, *25*, 2601–2604.
[14] A. Espinosa Ferao, *Inorg. Chem.* **2018**, *57*, 8058–8064.
[15] Z. Jie, V. Rammoorty, B. Fischer, *J. Org. Chem.* **2002**, *67*, 711–719.
[16] T. Krachko, E. Nicolas, A. W. Ehlers, M. Nieger, J. C. Slootweg, *Chem. Eur. J.* **2018**, *24*, 12669–12677.
[17] A. Espinosa Ferao, R. Streubel, *Inorg. Chem.* **2020**, *59*, 3110–3117.
[18] a) D. V. Deubel, *J. Am. Chem. Soc.* **2004**, *126*, 996–997; b) C. Schulten, G. von Frantzius, G. Schnakenburg, A. Espinosa, R. Streubel, *Chem. Sci.* **2012**, *3*, 3526–3533.
[19] a) J. P. Donahue, *Chem. Rev.* **2006**, *106*, 4747–4783; b) *NIST-JANAF Thermochemical Tables*, 4th edn. (Ed. M. W. Chase Jr.), American Chemical Society and the American Institute of Physics, Whasington DC, **1998**.
[20] K. P. Kepp, *Inorg. Chem.* **2016**, *55*, 9461–9470.
[21] R. Robiette, J. Richardson, V. K. Aggarwal, J. N. Harvey, *J. Am. Chem. Soc.* **2006**, *128*, 2394–2409.
[22] A. W. Kyri, F. Gleim, A. García Alcaraz, G. Schnakenburg, A. Espinosa Ferao, R. Streubel, *Chem. Commun.* **2018**, *54*, 7123–7126.
[23] a) I. Mayer, *Chem. Phys. Lett.* **1983**, *97*, 270–274; b) I. Mayer, *Int. J. Quantum Chem.* **1984**, *26*, 151–154; c) I. Mayer, *Theor. Chim. Acta* **1985**, *67*, 315–322; d) I. Mayer, in *Modelling of Structure and Properties of Molecules*, (Ed. Z. B. Maksic), John Wiley & sons, New York, Chichester, Brisbane, Toronto, **1987**; e) A. J. Bridgeman, G. Cavigliasso, L. R. Ireland, J. Rothery, *J. Chem. Soc. Dalton Trans.* **2001**, 2095–2108.
[24] a) H. S. He, C. W. Y. Chung, T. Y. S. But, P. H. Toy, *Tetrahedron* **2005**, *61*, 1385–1405; b) M. C. Henry, G. Wittig, *J. Am. Chem. Soc.* **1960**, *82*, 563–564; c) A. W. Johnson, *J. Org. Chem.* **1960**, *25*, 183–185; d) C. Raeck, S. Berger, *Eur. J. Org. Chem.* **2006**, *21*, 4934–4937.
[25] a) Y. Uchiyama, N. Kano, T. Kawashima, *J. Am. Chem. Soc.* **2003**, *125*, 13346–13347; b) T. Kawashima, Y. Uchiyama, N. Kano, *Phosphorus Sulfur Silicon Relat. Elem.* **2004**, *749*, 849–852.
[26] T. Maulbetsch, E. Jergens, D. Kunz, *Chem. Eur. J.* **2020**, *26*, 10634–10640.
[27] E. K. Moltzen, K. J. Klabunde, A. Senning, *Chem. Rev.* **1988**, *88*, 391–406.
[28] A. Espinosa Ferao, A. García Alcaraz, *New J. Chem.* **2020**, *44*, 8763–8770.
[29] S. Williamson, D. J. Michaelis, T. P. Yoon, *Chem. Rev.* **2014**, *114*, 8016–8036.
[30] a) R. W. Murray, R. Jeyaraman, *J. Org. Chem.* **1985**, *50*, 2847–2853; b) R. Mello, M. Fiorentino, O. Sciacovelli, R. Curci, *J. Org. Chem.* **1988**, *53*, 3890–3891; c) W. Adam, C.-G. Zhao, C. R. Saha-Möller, K. Jakka, *Oxidation of Organic Compounds by Dioxiranes"*, John Wiley & Sons Inc., **1990**; d) L. Zou, R. S. Paton, A. Eschenmoser, T. R. NewHouse, P. S. Baran, K. N. Houk, *J. Org. Chem.* **2013**, *78*, 4037–4048.

[31] A. Rey Planells, A. Espinosa Ferao, *Inorg. Chem.* **2022**, *61*, 13846–13857.
[32] A. Espinosa Ferao, A. Rey Planells, R. Streubel, *Eur. J. Inorg. Chem.* **2021**, *22*, 348–353.
[33] F. Neese. ORCA – an Ab Initio, DFT and Semiempirical SCF-MO Package. D-45470 Mülheim/Ruhr: Max Planck Institute for Bioinorganic Chemistry. Version 4.2.1. http://www.cec.mpg.de/forum/portal.php. F. Neese, *WIREs Comput. Mol. Sci.* **2017**, *8*, e1327.
[34] a) C. Lee, W. Yang, R. G. Parr, *Phys. Rev. B* **1988**, *37*, 785–789; b) A. D. Becke, *J. Chem. Phys.* **1993**, *98*, 5648–5652.
[35] a) F. Weigend, R. Ahlrichs, *Phys. Chem. Chem. Phys.* **2005**, *7*, 3297–3305; b) A. Schäfer, C. Huber, R. Ahlrichs, *J. Chem. Phys.* **1994**, *100*, 5829–5835.
[36] F. Neese, F. Wennmohs, A. Hansen, U. Becker, *Chem. Phys.* **2009**, *356*, 98–109.
[37] a) E. Caldeweyher, C. Bannwarth, S. Grimme, *J. Chem. Phys.* **2017**, *147*, 34112; b) E. Caldeweyher, S. Ehlert, A. Hansen, H. Neuegebauer, S. Spicher, C. Bannwarth, S. Grimme, *J. Chem. Phys.* **2019**, *150*, 154122.
[38] K. Ishida, K. Morokuma, A. Komornicki, *J. Chem. Phys.* **1977**, *66*, 2153–2156.
[39] a) V. Barone, M. Cossi, *J. Phys. Chem. A* **1998**, *102*, 1995–2001; b) M. Cossi, N. Rega, G. Scalmani, V. Barone, *J. Comb. Chem.* **2003**, *24*, 669–681.
[40] C. Riplinger, B. Sandhoefer, A. Hansen, F. Neese, *J. Chem. Phys.* **2013**, *139*, 134101.
[41] J. A. Pople, M. Head-Gordon, K. Raghavachari, *J. Chem. Phys.* **1987**, *87*, 5968.
[42] B. O. Roos, *Adv. Chem. Phys.* **1987**, *69*, 399–445.
[43] R. J. Gdanitz, R. Ahlrichs, *Chem. Phys. Lett.* **1988**, *143*, 413–420.

Manuscript received: August 24, 2023
Revised manuscript received: September 30, 2023
Accepted manuscript online: October 2, 2023
Version of record online: October 17, 2023